Multivalent Effects of RGD Peptides Obtained by Nanoparticle Display

Xavier Montet,[†] Martin Funovics,[‡] Karin Montet-Abou,[†] Ralph Weissleder,[§] and Lee Josephson*[,§]

Department of Radiology, Geneva Hospital, Geneva, Switzerland, Department of Angiography and Interventional Radiology, Vienna Medical University, Vienna, Austria, and Center for Molecular Imaging Research, Massachusetts General Hospital and Harvard Medical School, Charlestown, Massachusetts

Received May 2, 2006

The binding of RGD peptides to integrins offers an excellent system to study the multivalent mediated changes in affinity that arise when peptides, displayed on the surface of a nanoparticle carrier, bind to integrins displayed on the cell membrane. The IC50 of an RGD nanoparticle for endothelial adhesion was 1.0 nM nanoparticle or 20 nM peptide (20 peptide/nanoparticle) and was associated with strong multivalent effects, defined as a multivalent enhancement factor (MVE) of 38 (MVE = IC50 (peptide)/IC50 (peptide when displayed by nanoparticle)). The attachment of RGD peptides to nanoparticles resulted in an extension of the peptide blood half-life from 13 to 180 min. Based on the multivalent enhancement of affinity and extension of blood half-life, multivalent RGD nanoparticle-sized materials should be potent inhibitors of the alpha(V)beta(3) function on endothelial cells in vivo.

Introduction

The quest for more potent and selective diagnostic and therapeutic agents and widespread interest in nanotechnology have led to recent proposals that targeted nanoparticle-based pharmaceuticals might be designed to fit this need, see http://nano.cancer.gov/.[1] Compared to lower molecular weight pharmaceuticals, nanoparticles have both advantages (high detectability per mole of nanoparticle and multivalent interactions) and disadvantages (slow diffusion through tissues and withdrawal by macrophages/short blood half-life). While there is a large amount of literature covering many types of nanoparticles and their applications, few well-defined nanoparticles have been studied in detail, both in vivo and in vitro, to provide an understanding of the potential benefits and drawbacks of targeted nanoparticle-based therapeutic or diagnostic drugs. Our long-term goal has been to use a well-studied nanoparticle carrier and peptide/receptor system (aminated cross-linked iron oxide (CLIO), amino-CLIO and the RGD peptide/integrin-binding system) to study the advantages and disadvantages of targeted nanoparticles in vivo and in vitro. To that end, in vivo studies with a nanoparticle used in the current study, RGD-CLIO(med), have demonstrated the nanoparticle's ability to visualize integrins expressed on BT-20 tumor cells, that is, integrins expressed on tumor cells beyond the endothelial barrier by fluorescent or magnetic resonance based imaging. The ability to image integrins was a result of a high integrin expression on BT-20 tumor cells, a high tumor capillary density, and the ability of the nanoparticle to extravasate.[2] The goals of the current study were to use in vitro systems to determine the magnitude of multivalent effects resulting from the display of RGD peptides on nanoparticles with different cells and different types of assays.

In nature, multivalent interactions are often employed between the proteins displayed on the surface of one cell (e.g., integrins, selectins, cadherins, and intercellular adhesion molecules (ICAMs)) and small structures on the surface of an adjacent cell or the extracellular matrix (e.g., RGD motif and sialyl Lewis^X), to regulate cell migration and inflammatory processes. Surface-to-surface/ligand-to-receptor multivalent interactions are one of many distinct types of multivalent interactions found in nature, see Figure 2 of ref 3 and refs 4 and 5. The binding of integrins to RGD motifs on the extracellular matrix is through conformational changes, which alters the binding of monomeric peptides, and by clustering, which alters multivalent interactions sometimes termed avidity effects.[6−8] The distribution of integrins in the membrane changes in a dynamic manner, regulating multipoint attachment with RGD motifs and the strength of multivalent effects. When nanoparticles are used as carriers for the attachment of integrin-binding peptides, simultaneous binding between the multiple peptides and multiple extracellular integrin domains over an extended area of membrane can occur as shown in Figure 1. (The RGD-CLIO nanoparticle and extracellular integrin domain are considered to be spheres with diameters of 30 nm (Table 1) and 6 nm,[9] respectively, half of which can interact in a surface-to-surface mediated fashion.) The display of peptides by nanoparticle carriers offers the potential to design molecularly targeted materials that exploit surface-to-surface/ligand-to-receptor multivalent interactions.

We employed two types of assays to examine the interaction between RGD nanoparticles and cell-surface integrins. The first was an assay for cell-associated nanoparticles, which is useful in understanding the fate of a nanoparticle in the cell-based assay, and potentially in vivo, but gives no information on a material's pharmacological activity. However, because RGD nanoparticles can be used to image integrins,[2] their fate in vivo and correspondence between their fate in vivo and in vitro is of some interest. The second was an anti-adhesion assay, which is an often-used method of assessing the potency of RGD-based, anti-angiogenic pharmaceuticals.[10,11] The anti-adhesion assay was employed not only to understand nanoparticle-based multivalent interactions, but also to evaluate the potential of RGD nanoparticles to serve as a class of integrin-targeted therapeutic agents.

The uptake and anti-adhesion assays were then performed with alpha(V)beta(3) integrin-expressing endothelial cells and tumor cells. Alpha(V)beta(3) integrins are expressed on endothelial cells,[12] but they are also expressed on tumor cell lines[13]

* To whom correspondence should be addressed. Tel.: (617) 726-6478. Fax: (617) 726-5708. E-mail: ljosephson@partners.org.
[†] Geneva Hospital.
[‡] Vienna Medical University.
[§] Massachusetts General Hospital and Harvard Medical School.

10.1021/jm060515m CCC: $33.50
Published on Web 09/02/2006

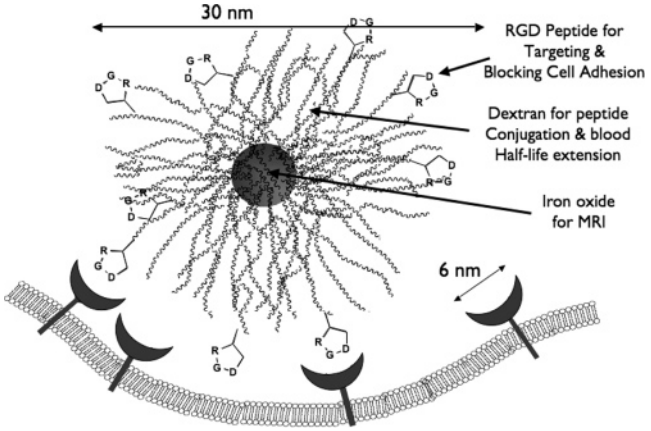

Figure 1. Surface-to-surface nanoparticle-based multivalent interactions. A peptide−nanoparticle conjugate bearing cRGD peptides provides a surface for simultaneous, multiple interactions with the cell surface, giving rise to multivalent effects. Functions of the components of the nanoparticle are given.

Table 1. Summary of Physical Properties of Nanoparticles

nanoparticle	RGD per nanoparticle	size (nm)	Cy5.5 per nanoparticle
RGD-CLIO(lo)	4.1	29 ± 5	7.2
RGD-CLIO(med)	20.0	30 ± 3	7.2
RGD-CLIO(hi)	52.0	39 ± 4	7.2

and a variety of cells that are not endothelial or epithelial in nature.[14,15] While the alpha(V)beta(3) integrin of endothelial cells is involved with adhesion to RGD motifs in the extracellular matrix (basement membrane),[16] the function of the same integrin on tumor cells could well be different from that of endothelial cells. Therefore, assays were performed on both alpha(V)beta(3) expressing endothelial and tumor cells.

The display of RGD peptides by nanoparticles resulted in strong multivalent interactions and low EC50s and IC50s that depended on the cell type and assay. In addition, the conjugation of RGD peptides to nanoparticles extended peptide blood half-life. Due to multivalent effects and blood half-extension, the display of integrin-binding pharmacophores by nanoparticles offers an approach to the design of pharmaceuticals that may work at substantially lower doses in vivo than their monovalent counterparts.

Materials and Methods

Peptide Synthesis: Fluoresceinated and nonfluoresceinated RGD peptides were synthesized as GSSK(Fl)GGGCRGDC and GSSK-GGGCRGDC with C-terminal amides by the Tufts Peptide Core Facility (Boston, MA). Fluorescein was attached to the peptide through the use of *N*-α-Fmoc-*N*-ϵ-(5-carboxyfluorescein)-L-lysine (Anaspec, San Jose, CA) during synthesis. Both peptides were cyclized at the cysteines (for the linkage see Figure 2) by oxidation (bubbling air, room temperature, 24 h) at less than 0.5 mg/mL peptide in 0.1 M ammonium bicarbonate. Cyclization was confirmed by mass spectrometry. The fluoresceinated, cyclized peptide was conjugated to nanoparticles, while the cyclic, unfluoresceinated GSSKGGGCRGDC peptide was used in Figure 6. The head-to-tail cyclic RGDfV peptide was from Bachem (Bachem, Torrance, CA). This peptide differs from cilengitide (EMD 121974 or cyclo-Arg-Gly-Asp-D-Phe-(*N*-methyl)-Val) by the addition of a methyl group.[10] Cilengitide is in clinical trials as an anti-angiogenic, anticancer agent.[17]

Nanoparticle Synthesis: Superparamagnetic iron oxide nanoparticles with an aminated, cross-linked dextran coating were synthesized as described[18,19] and used to synthesize the three RGD nanoparticles at three different valencies. The general synthesis of RGD nanoparticles is shown in Figure 2, with the procedure for the synthesis of the cyclic RGD (cRGD)-CLIO(med) given. To 100 μL of 100 mM suberic acid bis(*N*-hydroxysuccinimide ester) or DSS (Pierce Chemical, Rockford, IL; 10 μmoles) in DMF was added 5 μL of diisopropylethylamine (0.39 μmoles). Then 1 mM **1** cRGD peptide in 40 μL of DMF (40 nmoles) was added in 5 μL portions. The mixture was incubated (1 h, 25 °C), and NHS-activated cRGD peptide, **2**, was precipitated with 800 μL of *m*-terbutyl ether. To the precipitate was added amino-CLIO, **3**, (100 μL, 5 mg of Fe/mL, (1.1 nmole particles, 72 nmoles amine at 160 amines/8000 Fe and 8000 Fe/nanoparticle), and the mixture was allowed to sit overnight. Unreacted peptide was removed using a PD-10 column. To synthesize RGD-CLIO(hi) or RGD-CLIO(lo), 1 mM cRGD peptide was added in a volume of 120 μL (120 nmoles) or 15 μL (15 nmoles), respectively.

Nanoparticle Characterization: The average number of peptides attached per nanoparticle was determined spectrophotometrically from fluorescein absorbance.[19] Numbers of peptides per nanoparticle were expressed based on 8000 iron atoms per amino-CLIO nanoparticle, obtained by the viscosity/light scattering method for nanoparticle core weights.[20] Size was determined by laser light scattering (Zetasizer, Malvern Instruments, Malvern, PA). Relaxivities were determined at 20 mHz and 40 °C using a Bruker Minispec 20 (Bruker Instruments, Billerica, MA). The physical properties of the cRGD-CLIO(lo), **4**, cRGD-CLIO(med), **5**, and cRGD-CLIO(hi), **6**, are summarized in Table 1.

The BT-20 cells were from the American Tissue Culture Collection (Manassas, VA) and cultured according to the manufacturer's instructions. Human umbilical vein endothelial cells (HUVECs, Clonetics, Baltimore, MD) were cultured in endothelial growth medium (Clonetics, Baltimore, MD). Values of EC50 and IC50 were determined from four parameter fits using GraphPad Prism (GraphPad Software, San Diego, CA).

Peptide and Nanoparticle Uptake Assays: To determine cell associated RGD peptide or peptide-nanoparticle, BT-20 cells were incubated with various peptide or peptide-nanoparticle concentrations in the media above (30 min, 37° C, 5% CO_2) in six well plates at about 1 million cells per well. Cells were then washed three times with Hank's Balanced Salt Solution (HBSS; Mediatech, Inc., Herndon, VA) and lysed with phosphate-buffered saline containing 0.1% Triton-X100 and 1 mM 8-anilino-1-naphthalenesulfonic acid. Because the fluorescein is covalently attached to the cRGD peptide, see Figure 2, the same assay for cell-associated fluorescein can be used to quantitate either a cell-associated peptide or a cell-associated nanoparticle. Fluorescein was measured by an immunoassay using microtiter plates coated with fluorescein−albumin and a horseradish peroxidase anti-fluorescein conjugate.[21]

Anti-Adhesion Assay: Cells were grown to a subconfluent state and harvested by 0.025% trypsin/EDTA. Cells (2×10^4 cells/100 μL/well) were incubated with various concentrations of cRGD, cRGDfV, or nanoparticle on ice for 15 min and then placed into a 96-well microtiter plate, which was coated with vitronectin (500 ng/well). CLIO was also added to cells as controls. After a 1 h incubation at 37 °C and 5% CO_2, unattached cells were gently removed by rinsing the wells with HBSS. Attached cells were fixed in 4% paraformaldehyde and stained with 3% crystal violet. The optical density at 562 nm was read on an Emax microtiter plate reader (Molecular Devices, Sunnyvale, CA). Data points for the anti-adhesion and uptake assays were obtained in triplicate. Values of EC50 or IC50 are the average of at least two determinations, with uncertainty recorded as the standard error. EC50 is the effective concentration for 50% of maximum uptake. IC50 is the concentration for 50% inhibition of cell adhesion.

For determination of blood half-life by intravital microscopy, 10 nmoles of fluorescein as peptide or nanoparticle were injected by tail vein into nude mice. After median laparotomy, a section of sigmoid colon was exposed and imaged using a multichannel Radiance 2100 system (Bio-Rad, Richmond, CA). The fluorescence inside the vessel was recorded over time by operator-defined regions of blood vessel intensity, which were distinguishable from interstitial fluorescence by clearly defined anatomical margins. The blood half-

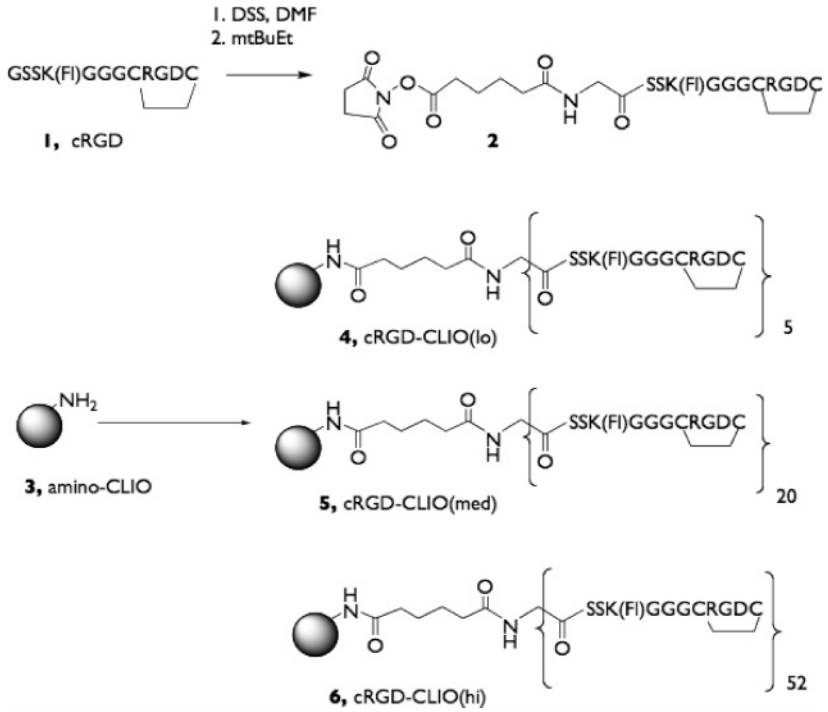

Figure 2. Synthesis of cRGD-CLIO nanoparticles with different numbers of peptides attached. The primary amine of the cRGD peptide is reacted with DSS, precipitated with *m*-terbutyl ether, and reacted with the amino-CLIO nanoparticle. Different amounts of peptide are reacted with the nanoparticle to obtain nanoparticles with different numbers of peptides attached. Fluorescein attached to the epsilon amine of lysine is denoted K(Fl).

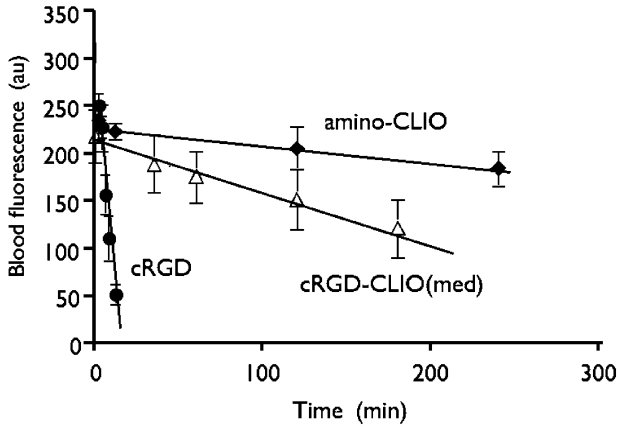

Figure 3. Blood half-lives of the cRGD peptide, amino-CLIO nanoparticle. and cRGD-CLIO(med) nanoparticle. Time-dependence of blood vessel fluorescence was determined by intravital microscopy. Attaching the peptide to amino-CLIO results in a decrease in blood half-life, but the cRGD-CLIO(med) nanoparticle has a far longer blood half-life than the cRGD peptide.

life was determined by fitting the data to a single-exponential equation using GraphPad Prism (GraphPad Software, San Diego, CA). Uncertainties, that is, standard errors, were given by the fitting procedure.

Results

The utility of peptide-nanoparticles as molecularly targeted agents depends in large measure on the ability of the attached peptide to bind a molecular target and govern the interaction between the nanoparticle and the cells. In vitro and in vivo experiments indicate the cRGD-CLIO(med) nanoparticle interacts with cells through the cRGD peptide and not via nonspecific nanoparticle/cell interactions.

Affinity Shift with Change of Peptide Conformation (in vitro): An advantage of using the disulfide-linked cRGD peptide for the synthesis of peptide-nanoparticle conjugates is that it permits a demonstration of the specificity of the interaction between nanoparticles and cells through the peptide by the increase in EC50 or IC50 accompanying the conversion of a cRGD peptide to a linear RGD peptide. For example, dithiothreitol treatment of cRGD-CLIO(med) caused a 38-fold increase in the EC50 for nanoparticle uptake with BT-20 cells (0.011 μM to 0.40 μM, see Figure 2B of ref 2[2]). The RGD sequence is found in the loops of proteins,[22] and cRGD peptides have roughly 10−100 higher affinities for their receptors than corresponding linear forms.[23,24]

Differential Binding to Cell Lines (in vitro): We measured the binding of the cRGD peptide to BT-20 and 9L cell lines in vitro (Figure 2C of ref 2[2]); the BT-20 tumor bound 0.82 picomoles of cRGD peptide (1 million cells) compared to the 0.16 pico molecules for the 9L tumor. The presence of alpha-(V)beta(3) integrin on BT-20 tumor cells was established by the binding of fluorescein-labeled cRGD peptide and Cy5.5-labeled anti-alpha(V)beta(3) antibody using dual wavelength FACS.[2] The antibody binds alpha(V)beta(3) integrin on BT-20 tumors.

Lack of Effects of the Amino-CLIO Precursor Nanoparticle on Uptake and Cell Adhesion Assays (in vitro): The amino-CLIO nanoparticles, the nanoparticle used for peptide attachment, had no effect on the anti-adhesion assay and were not internalized by cells at 100 μg Fe/mL, which exceeds the concentrations of the RGD nanoparticles employed.

Targeting of cRGD-CLIO(med) to the Integrin Expressing BT-20 Tumor (in vivo): We measured the uptake of intravenously injected cRGD-CLIO nanoparticles with implanted BT-20 and 9L tumors (Figure 3 of ref 2[2]). RGD-peptide mediated nanoparticle uptake was seen with the BT-20 tumor and not with the 9L tumor or with other normal tissues.

Long Blood Half-Life of the Amino-CLIO Precursor Nanoparticles (in vivo): The amino-CLIO nanoparticle used for peptide attachment has a blood half-life of 508 min (Figure

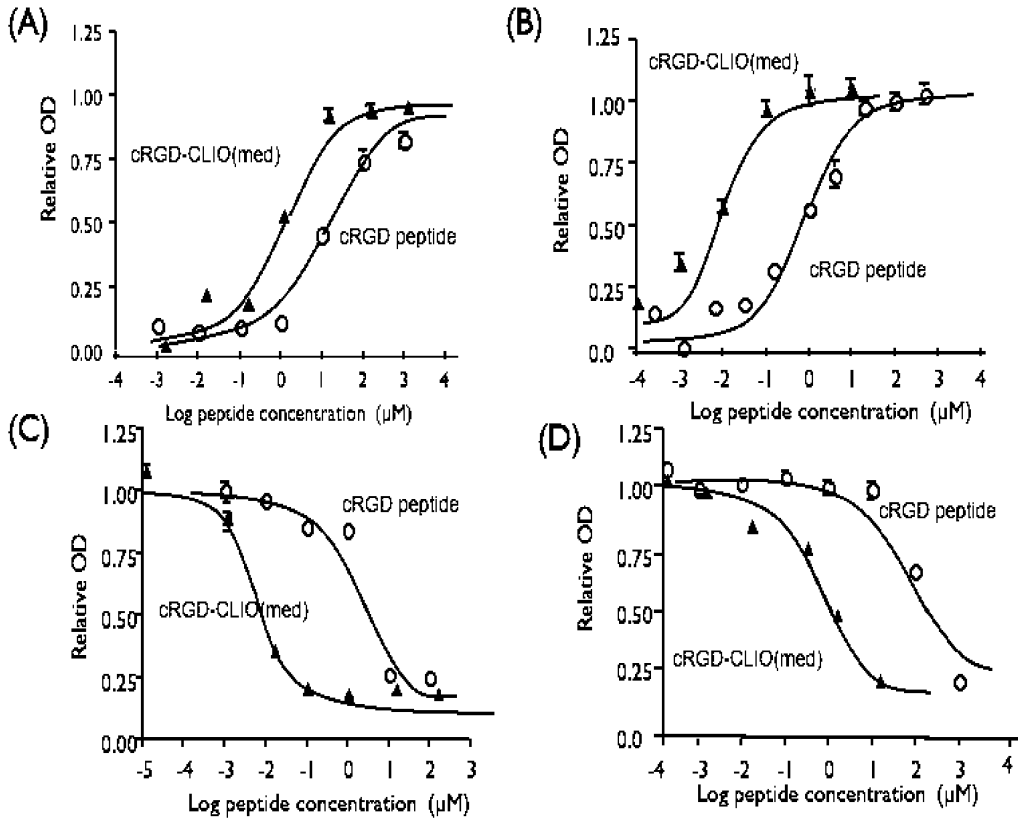

Figure 4. Uptake and anti-adhesion assays with the cRGD peptide and cRGD-CLIO(med) nanoparticle. Two types of assays with two cell types are shown: (A) uptake assay with HUVECs; (B) uptake assay with BT-20 tumor cells; (C) anti-adhesion assay with HUVECs; and (D) anti-adhesion assay with BT-20 tumor cells.

Table 2. Multivalent Enhancement (MVE) of cRGD-CLIO Nanoparticles with HUVECs and BT-20 Cells[a]

	HUVEC				
	cRGD peptide (uM)	cRGDfV peptide	cRGD-CLIO(lo)	cRGD-CLIO(med)	cRGD-CLIO(hi)
uptake EC50	6.0 ± 2.1	NA[b]	5.9 ± 2.2	1.58 ± 0.26	5.63 ± 3.0
uptake MVE	1.0	NA[b]	0.98	3.8	1.07
anti-adhesion IC50	0.76 ± 0.34	0.125 ±0.04	0.030 ± 0.012	0.020 ± 0.002	0.12 ± 0.09
anti-adhesion MVE	1.0	NA[b]	25.3	38.0	6.3
	BT-20				
	peptide (cRGD)	peptide cRGDfV	cRGD-CLIO(lo)	cRGD-CLIO(med)	cRGD-CLIO(hi)
uptake EC50	1.20 ± 0.3	NA[b]	0.047 ± 0.021	0.011 ±0.005	0.068 ±0.029
uptake MVE	1.0	NA[b]	25.5	109	17.6
anti-adhesion IC50	130 ± 21	41 ± 22	7.43 ±2.53	1.82 ± 0.4	5.34 ±2.87
anti-adhesion MVE	1.0	NA[b]	17.4	71.4	24.3

[a] Concentrations are expressed as mean ±1 SD in units of micromolar peptide, as shown in Figure 4, and MVE is the IC50 (or EC50) of the cRGD peptide divided by the IC50 of the cRGD-CLIO nanoparticle. [b] NA, not available.

3) due to very poor recognition of the nanoparticle by macrophages of the reticuloendothelial system. Attachment of the RGD peptide reduced blood half-life, modestly, to 180 min. The inability of cells to bind to amino-CLIO is due to the thick hydrophilic coating of cross-linked dextran (Figure 1), which gives the nanoparticle a "stealth-like capability," that is, an inability to be recognized by cells. Attachment of the cRGD peptide then causes the nanoparticle to be recognized by integrins and blood half-life decreases.

Figure 4A,B shows typical uptake curves for the cRGD peptide both in its monovalent state, that as a peptide, and in its multivalent state, that is, as displayed on cRGD-CLIO(med), by HUVECs and BT-20 cells, respectively. Figure 4C,D shows typical curves for the inhibition of cell adhesion to vitronectin-coated plates by the monovalent cRGD peptide and when that peptide was displayed by the multivalent cRGD-CLIO(med) nanoparticle, again with HUVECs and BT-20 cells, respectively. With both cell types and assays, the cRGD peptide, when displayed by the nanoparticle, was active at lower concentrations than the parent peptide. Data were fit to a four-parameter equation to obtain EC50s for uptake and IC50s for the inhibition of adhesion, with values, and those of the associated multivalent enhancement ratios (MVEs), shown in Table 2. Values are expressed as micromolar concentrations of peptide for both monomeric peptide and multivalent nanoparticle.

To evaluate the strength of multivalent enhancement with the RGD/integrin system, we used the multivalent enhancement ratio, which was obtained by dividing the IC50 (or EC50) for the monovalent cRGD peptide by the IC50 (or EC50) of the multivalent cRGD peptide-nanoparticle. The MVE expresses multivalent interactions as the apparent dissociation constant in the multivalent state, divided by the apparent affinity constant in the monomeric state; it is the multivalent "affinity" normalized to monovalent affinity. The MVE permits a comparison

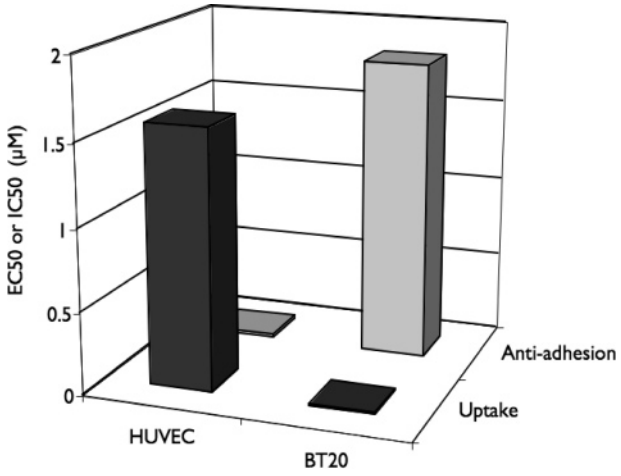

Figure 5. Interactions of cRGD-CLIO(med) nanoparticles with BT20 tumor cells and endothelial cells. HUVECs have a low IC50 in the anti-adhesion assay and a high EC50 in the uptake assay, while the opposite is true for BT-20 cells.

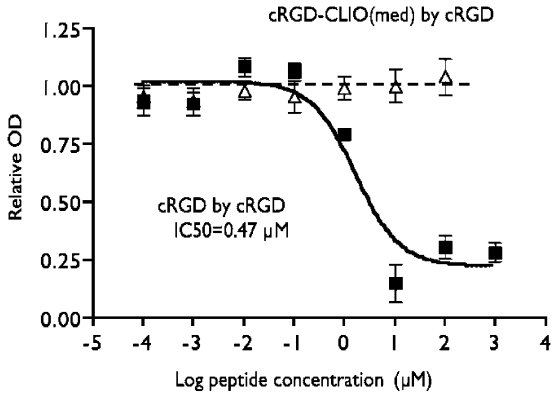

Figure 6. Inability of a cRGD peptide to inhibit uptake of the cRGD-CLIO(med) nanoparticle by BT20 cells. The *monovalent* cRGD peptide cannot inhibit uptake of the *multivalent* cRGD-CLIO(med) nanoparticle (triangles). A *monovalent* nonfluoresceinated cRGD peptide inhibits the uptake of the *monovalent* fluoresceinated monovalent peptide, cRGD (squares).

of strength of multivalent effects when RGD peptides are attached to nanoparticles at different densities. It can also be used to compare multivalent effects when different types of RGD peptide or peptidomimetics, with differing IC50s as monomeric materials, are attached to nanoparticles at a similar density.

As shown in Table 2, the cRGD-CLIO(med) nanoparticle had stronger multivalent effects than cRGD-CLIO(lo) or cRGD-CLIO(hi) with both cell types and both types of assays. With HUVECs, the IC50 (anti-adhesion) was substantially lower than the EC50 (uptake). However, with BT-20 cells, the opposite pattern was obtained, with the EC50 (uptake) being substantially lower than the IC50 (anti-adhesion), a situation that is summarized in Figure 5. HUVECs required high concentrations of the cRGD peptide or the cRGD-CLIO nanoparticles for internalization, but were quite *sensitive to their anti-adhesive effects*. On the other hand, BT-20 tumor cells *internalized* cRGD peptides or cRGD nanoparticles at low concentrations but were *insensitive* to their anti-adhesive effects.

Multivalent effects can be expressed in two ways, either per mole of attached peptide or per mole of nanoparticle. The MVE of cRGD-CLIO(med) of 38.0 (Table 2) yields a value of 760 (38 at 20 peptides/nanoparticle) for the improved in vitro potency on a molar nanoparticle basis. Similarly, if the IC50 were expressed per mole of nanoparticle, a 20-fold reduction of the IC50 per peptide (from 0.020 μM to 1.0 nM) would be obtained. The latter value is comparable to some of the dissociation constants obtained with optimized, low molecular weight alpha(V)beta(3) antagonists.[10,25]

A feature of simultaneous interactions between multiple RGD motifs and multiple integrins is that monovalent ligands will be poor inhibitors, because the monovalent ligand must simultaneously block all of the many RGD nanoparticle/integrin interactions to block nanoparticle/membrane association.[26] To test this prediction, we attempted to inhibit the uptake of cRGD-CLIO(med) by BT-20 cells, which had an MVE of 109 (Table 2), with a monovalent cRGD peptide. As shown in Figure 6, a cRGD peptide failed to block nanoparticle uptake, but clearly inhibited the uptake of the monovalent cRGD peptide with an IC50 of 0.47 μM, which compared reasonably well to the EC50 for uptake of 1.20 μM. For this reason, we employed a disulfide-linked cyclic peptide, cRGD, in the synthesis of our nanoparticles and relied on the dithiothreitol-induced increase in an IC50 or EC50 to indicate that nanoparticle−cell interactions were mediated by integrin binding.

The possible rapid clearance of nanoparticles in vivo could substantially reduce the increased potency achieved by multivalent effects evident with in vitro assays. It was, therefore, of interest to compare the blood half-life of the cRGD peptide and cRGD-CLIO(med) nanoparticle, which were determined using vessel fluorescence by intravital microscopy, as shown in Figure 3. The cRGD-CLIO(med) had a blood half-life of 180 min, compared with 13 min for the cRGD peptide. As a control, the half-life of the parent amino-CLIO nanoparticle was found to be 508 min, which is in good agreement with the blood half-life of 640 min, determined using a radioactive nanoparticle.[27]

Discussion

With the RGD/integrin system, the MVE is a useful method of denoting the strength of multivalent interactions. RGD/integrin binding uses modest affinity constants (10^5-10^7 M^{-1}) but involves many integrins on the cell surface and simultaneous binding to RGD motifs displayed over a wide area of the extracellular matrix.[28,29] The regulation of the binding of integrins to RGD motifs is by integrin conformational changes, which alters the affinity of integrins for monomeric peptides, and by varying the distribution of integrins within the plane of the membrane.[6,7] The MVE defines the multivalent interactions of peptide-nanoparticles by using values normalized for changes in the binding of monomeric peptides, thereby taking into account differences in the affinity for monomeric peptides present with the integrin system.

Depending on the assay and cell type, cRGD-CLIO(med) nanoparticle had a wide range of EC50s, IC50s, and MVEs. HUVECs were sensitive to the anti-adhesive effects of cRGD-CLIO(med) (IC50 = 0.020 μM) but internalized the nanoparticles poorly (EC50 = 1.58 μM), a difference associated with large differences in MVE (38 versus 3.8). On the other hand, BT-20 tumor cells were insensitive to the anti-adhesive effects of cRGD-CLIO(med) (IC50 = 1.82 μM), while internalizing the nanoparticle avidly (EC50 = 0.011 μM). Here variations of nanoparticle EC50 reflected differences in the EC50 for the monomeric peptides because values of the MVE were high and similar (109 and 71, respectively). The relative EC50 values we obtained were consistent with the behavior of cRGD-CLIO-(med) after injection: the low EC50 of the BT-20 tumor cell in vitro is consistent with the observed accumulation of cRGD-CLIO(med) in a tumor rather than in endothelial cells in vivo.[2]

Differences in the MVE likely reflect the ability of cells to alter integrin affinity through changes in integrin affinity and distribution within the membrane.[6−8]

The model of multivalency resulting from simultaneous interactions between RGD peptides on a nanoparticle and the integrins on a cell membrane (Figure 1) has several features consistent with our data. First, strong multivalent interactions can occur with relatively few peptides per nanoparticle, much as strong multivalent interactions require only a divalency of antibodies.[26,30] In fact, MVEs for cRGD-CLIO(lo) at four peptides/30 nm nanoparticle were 25.3 (HUVEC/anti-adhesion) and 25.5 (BT-20/uptake), see Table 2. Second, when the density of RGD peptides on the nanoparticle exceeds the density of RGD/integrin-binding sites displayed by the membrane, the "extra" peptides displayed by the nanoparticle cannot participate in integrin binding. There is one RGD binding site per integrin molecule, and each integrin molecule is approximately equivalent to a 6-nm diameter sphere, based on the crystal structure of the RGD−integrin complex.[9] These features limit the maximum density of RGD binding sites on the membrane that can be obtained. The value of the MVE will, therefore, decrease (Table 2) when the density of peptides attached to nanoparticles exceeds the density of peptide binding integrins. Third, as a consequence of multivalent affinity enhancement, the monovalent cRGD peptide is unable to inhibit the uptake of multivalent RGD nanoparticles (Figure 6). For this reason, we relied on loss of apparent affinity obtained by linearization of the cRGD peptide with dithiothreitol as a proof that cRGD-CLIO(med) nanoparticles are interacting with integrins. Fourth, the model predicts that micron-sized particles, which offer a larger surface per particle than that of nanoparticles, could produce even larger MVEs. However, this prediction was not tested, because the molecular targeting of micron-sized carriers in vivo is limited by the reticuloendothelial system, which phagocytizes micron-sized particles faster than nanoparticles.[31−33] A variety of multivalent integrin-binding ligands have been synthesized using chemical scaffolds that are smaller than the nanoparticles used here and may not be as amenable to extended surface-to-surface-mediated multivalency.[11,34−37] Others have employed nanoparticle or particle carriers in the design of integrin-binding materials but have not characterized the strength of multivalent interactions.[38−40]

Based on the advantages of attaching RGD peptides to nanoparticles (strong multivalent interactions and extended blood half-life), the design of nanoparticles as nanoparticle carriers for eventual clinical use should be considered. If we combine the MVE effect (MVE = 38.0, Table 2) with the 15-fold extension of plasma half-life (13−180 min, Figure 3), attaching the cRGD peptide to the amino-CLIO nanoparticle could yield a form of the cRGD peptide with considerably greater anti-angiogenic activity than the low molecular weight peptide. Though the amino-CLIO nanoparticle, used to synthesize cRGD-CLIO(med), serves as a useful nanoparticle for understanding the multivalent effects in vitro and the fate of an RGD nanoparticle in vivo by imaging, an integrin-binding nanoparticle targeting alpha(V)beta(3) and used as an anti-angiogenic agent might lack the reporter iron oxide and reporter fluorochrome. A clinically useful nanoparticle carrier for pharmacophore attachment, in addition to permitting surface modification, would have to be nontoxic, amenable to terminal or filter sterilization, stable for years, and, once injected, breakdown to yield components that are excreted or metabolized. Development of such a nanoparticle carrier might then be employed as a platform for the attachment of monovalent materials that block cell-to-cell or cell-to-extracellular matrix interactions involving integrin or nonintegrin membrane proteins (selectins, cadherins, and ICAMs).

Acknowledgment. This study was supported by NIH Grants P50 CA86355, R24 CA92782, and R01 EB00662. X.M. was supported by a fellowship from the Swiss National Science Foundation (PBGEB-104665). K.M.A. was supported by the Swiss National Science Foundation (Grant PPOB-68778).

References

(1) Ferrari, M. Cancer nanotechnology: opportunities and challenges. *Nat. Rev. Cancer* **2005**, *5* (3), 161−171.
(2) Montet, X.; Montet-Abou, K.; Reynolds, F.; Weissleder, R.; Josephson, L. Nanoparticle imaging of integrins on tumor cells. *Neoplasia (N.Y.)* **2006**, *8* (3), 214−222.
(3) Kitov, P. I.; Bundle, D. R. On the nature of the multivalency effect: a thermodynamic model. *J. Am. Chem. Soc.* **2003**, *125* (52), 16271−16284.
(4) Mammen, M.; Chio, S.-K.; Whitesides, G. M. Polyvalent interactions in biological systems: implications for design and use of multivalent ligands and inhibitors. *Angew. Chem., Int. Ed.* **1998**, *37* (20), 2755−2794.
(5) Wright, D.; Usher, L. Multivalent binding in the design of bioactive compounds. *Curr. Org. Chem.* **2001**, *5* (11), 1107−1131.
(6) Carman, C. V.; Springer, T. A. Integrin avidity regulation: are changes in affinity and conformation underemphasized? *Curr. Opin. Cell Biol.* **2003**, *15* (5), 547−56.
(7) Zanetti, A.; Conforti, G.; Hess, S.; Martin-Padura, I.; Ghibaudi, E.; Preissner, K. T.; Dejana, E. Clustering of vitronectin and RGD peptides on microspheres leads to engagement of integrins on the luminal aspect of endothelial cell membrane. *Blood* **1994**, *84* (4), 1116−1123.
(8) Fernandez, C.; Clark, K.; Burrows, L.; Schofield, N. R.; Humphries, M. J. Regulation of the extracellular ligand binding activity of integrins. *Front. Biosci.* **1998**, *3*, 684−700.
(9) Xiong, J. P.; Stehle, T.; Goodman, S. L.; Arnaout, M. A. New insights into the structural basis of integrin activation. *Blood* **2003**, *102* (4), 1155−1159.
(10) Dechantsreiter, M. A.; Planker, E.; Matha, B.; Lohof, E.; Holzemann, G.; Jonczyk, A.; Goodman, S. L.; Kessler, H. *N*-Methylated cyclic RGD peptides as highly active and selective alpha(V)beta(3) integrin antagonists. *J. Med. Chem.* **1999**, *42* (16), 3033−3040.
(11) Kok, R. J.; Schraa, A. J.; Bos, E. J.; Moorlag, H. E.; Asgeirsdottir, S. A.; Everts, M.; Meijer, D. K.; Molema, G. Preparation and functional evaluation of RGD-modified proteins as alpha(v)beta(3) integrin directed therapeutics. *Bioconjugate Chem.* **2002**, *13* (1), 128−135.
(12) Ruoslahti, E. Specialization of tumour vasculature. *Nat. Rev. Cancer* **2002**, *2* (2), 83−90.
(13) Cheresh, D. A.; Smith, J. W.; Cooper, H. M.; Quaranta, V. A novel vitronectin receptor integrin (alpha v beta x) is responsible for distinct adhesive properties of carcinoma cells. *Cell* **1989**, *57* (1), 59−69.
(14) Singer, I. I.; Scott, S.; Kawka, D. W.; Kazazis, D. M.; Gailit, J.; Ruoslahti, E. Cell surface distribution of fibronectin and vitronectin receptors depends on substrate composition and extracellular matrix accumulation. *J. Cell Biol.* **1988**, *106* (6), 2171−2182.
(15) Westlin, W. F. Integrins as targets of angiogenesis inhibition. *Cancer J.* **2001**, *7* (Suppl 3), S139−143.
(16) Ruoslahti, E. Fibronectin and its integrin receptors in cancer. *Adv. Cancer Res.* **1999**, *76*, 1−20.
(17) Raguse, J.-D.; Gath Hans, J.; Bier, J.; Riess, H.; Oettle, H. Cilengitide (EMD 121974) arrests the growth of a heavily pretreated highly vascularised head and neck tumour. *Oral Oncol.* **2004**, *40* (2), 228−230. FIELD Journal Code: 9709118.
(18) Josephson, L.; Perez, J. M.; Weissleder, R. Magnetic nanosensors for the detection of oligonucleotide sequences. *Angew. Chem., Int. Ed.* **2001**, *40* (17), 3204−3206.
(19) Josephson, L.; Tung, C. H.; Moore, A.; Weissleder, R. High-efficiency intracellular magnetic labeling with novel superparamagnetic-Tat peptide conjugates. *Bioconjug. Chem.* **1999**, *10* (2), 186−191.
(20) Reynolds, F.; O'Loughlin, T.; Weissleder, R.; Josephson, L. Method of determining nanoparticle core weight. *Anal. Chem.* **2005**, *77* (3), 814−817.
(21) Kelly, K. A.; Reynolds, F.; Weissleder, R.; Josephson, L. Fluorescein isothiocyanate-hapten immunoassay for determination of peptide-cell interactions. *Anal. Biochem.* **2004**, *330* (2), 181−185.

(22) Kuhn, K.; Eble, J. The structural bases of integrin-ligand interactions. *Trends Cell Biol.* **1994**, *4* (7), 256−261.
(23) Aumailley, M.; Gurrath, M.; Muller, G.; Calvete, J.; Timpl, R.; Kessler, H. Arg-Gly-Asp constrained within cyclic pentapeptides. Strong and selective inhibitors of cell adhesion to vitronectin and laminin fragment P1. *FEBS Lett.* **1991**, *291* (1), 50−54.
(24) Haubner, R.; Gratias, R.; Diefenbach, B.; Goodman, S. L.; Jonczyk, A.; Kessler, H. Structural and functional aspects of RGD-containing cyclic pentapeptides as highly potent and selective integrin alphaV-beta3 antagonists. *J. Am. Chem. Soc.* **1996**, *118* (32), 7461−7472.
(25) Goodman, S. L.; Hoelzemann, G.; Sulyok, G. A. G.; Kessler, H. Nanomolar small molecule inhibitors for avb6, avb5, and avb3 integrins. *J. Med. Chem.* **2002**, *45* (5), 1045−1051.
(26) Munson, P. J.; Rodbard, D. Computer modeling of several ligands binding to multiple receptors. *Endocrinology* **1979**, *105* (6), 1377−1381.
(27) Wunderbaldinger, P.; Josephson, L.; Weissleder, R. Tat peptide directs enhanced clearance and hepatic permeability of magnetic nanoparticles. *Bioconjugate Chem.* **2002**, *13* (2), 264−268.
(28) Buck, C. A.; Horwitz, A. F. Cell surface receptors for extracellular matrix molecules. *Annu. Rev. Cell Biol.* **1987**, *3*, 179−205.
(29) Ruoslahti, E. RGD and other recognition sequences for integrins. *Annu. Rev. Cell Dev. Biol.* **1996**, *12*, 697−715.
(30) Crothers, D. M.; Metzger, H. The influence of polyvalency on the binding properties of antibodies. *Immunochemistry* **1972**, *9* (3), 341−357.
(31) Gaur, U.; Sahoo, S. K.; De, T. K.; Ghosh, P. C.; Maitra, A.; Ghosh, P. K. Biodistribution of fluoresceinated dextran using novel nanoparticles evading reticuloendothelial system. *Int. J. Pharm.* **2000**, *202* (1−2), 1−10.
(32) Chouly, C.; Pouliquen, D.; Lucet, I.; Jeune, J. J.; Jallet, P. Development of superparamagnetic nanoparticles for MRI: effect of particle size, charge and surface nature on biodistribution. *J. Microencapsulation* **1996**, *13* (3), 245−255.
(33) Awasthi, V. D.; Garcia, D.; Goins, B. A.; Phillips, W. T. Circulation and biodistribution profiles of long-circulating PEG-liposomes of various sizes in rabbits. *Int. J. Pharm.* **2003**, *253* (1−2), 121−132.
(34) Garanger, E.; Boturyn, D.; Jin, Z.; Dumy, P.; Favrot, M. C.; Coll, J. L. New multifunctional molecular conjugate vector for targeting, imaging, and therapy of tumors. *Mol. Ther.* **2005**, *12*(6), 1168−1175.
(35) Ye, Y.; Bloch, S.; Xu, B.; Achilefu, S. Design, synthesis, and evaluation of near-infrared fluorescent multimeric RGD peptides for targeting tumors. *J. Med. Chem.* **2006**, *49*, 2268−2275.
(36) Boturyn, D.; Coll, J. L.; Garanger, E.; Favrot, M. C.; Dumy, P. Template assembled cyclopeptides as multimeric system for integrin targeting and endocytosis. *J. Am. Chem. Soc.* **2004**, *126* (18), 5730−5739.
(37) Thumshirn, G.; Hersel, U.; Goodman, S. L.; Kessler, H. Multimeric cyclic RGD peptides as potential tools for tumor targeting: solid-phase peptide synthesis and chemoselective oxime ligation. *Chemistry* **2003**, *9* (12), 2717−2725.
(38) Anderson, S. A.; Rader, R. K.; Westlin, W. F.; Null, C.; Jackson, D.; Lanza, G. M.; Wickline, S. A.; Kotyk, J. J. Magnetic resonance contrast enhancement of neovasculature with alpha(v)beta(3)-targeted nanoparticles. *Magn. Reson. Med.* **2000**, *44* (3), 433−439.
(39) Hood, J. D.; Bednarski, M.; Frausto, R.; Guccione, S.; Reisfeld, R. A.; Xiang, R.; Cheresh, D. A. Tumor regression by targeted gene delivery to the neovasculature. *Science* **2002**, *296* (5577), 2404−2407.
(40) Schmieder, A. H.; Winter, P. M.; Caruthers, S. D.; Harris, T. D.; Williams, T. A.; Allen, J. S.; Lacy, E. K.; Zhang, H.; Scott, M. J.; Hu, G.; Robertson, J. D.; Wickline, S. A.; Lanza, G. M. Molecular MR imaging of melanoma angiogenesis with alpha(nu)beta(3)-targeted paramagnetic nanoparticles. *Magn. Reson. Med.* **2005**, *53* (3), 621−627.

JM060515M